Microscopic theory of critical folding nuclei and reconfiguration activation barriers in folding proteins

Shoji Takada and Peter G. Wolynes
School of Chemical Sciences, University of Illinois, Urbana, Illinois 61801

(Received 18 June 1997; accepted 4 September 1997)

An explicit droplet calculation is developed to address two aspects of the folding kinetics of large proteins: the thermodynamic folding barrier and the reconfiguration rate. First, a nonspecific folding nucleus is described as the instanton or droplet solution of a free energy functional derived for a minimally frustrated polymer Hamiltonian of the Gō type. Second, a theory for the barriers for transitions between trapped misfolded states is developed using a replica approach extended to inhomogeneous cases near the glass transition temperature of a random heteropolymer. Replica instantons are computed and their shape described. These two factors are then combined to give a microscopic theory of the folding time. © *1997 American Institute of Physics.* [S0021-9606(97)50646-5]

I. INTRODUCTION

Protein folding is a problem not only of stability but also of kinetics. The folding process can be viewed as an extremely complex chemical reaction from the reactant, unfolded states, to the product, the native state.[1] For a small protein, a globally defined reaction coordinate, e.g., the number of native pair contacts, has been used to describe the folding free energy profile and to estimate rates. There, the Kramers rate theory has been extended to take into account the ruggedness in the free energy landscape.[1,2] Simply, the folding time τ_F can be written as

$$\tau_F = \tau e^{\beta F^{\ddagger}}, \tag{1}$$

where τ is a time scale for reconfiguration of a protein in the reaction coordinate, and $F^{\ddagger}$ is a free energy barrier for the folding transition. At a relatively high temperature, the folding rate is largely governed by $F^{\ddagger}$ as in the ordinary transition state theory. As temperature decreases, the ruggedness of the free energy landscape becomes more important and τ becomes larger and larger, as in glassy materials.

For larger proteins, while a single reaction coordinate, or one order parameter, may be sufficient, its microscopic character changes to some extent. Instead of a uniform acquisition of structure, we can easily think of a situation where a portion of protein has folded while the rest is still unfolded. This heterogeneity may appear as an intermediate state that describes a folding domain or as a transition state. The latter, usually called a critical folding nucleus, diminishes the folding barrier $F^{\ddagger}$ estimated from the uniform mean field description. Likewise in escaping a kinetic trap, a local portion of a protein may reconfigure from one metastable non-native minimum to another. The rate of the escape determines the reconfiguration rate τ mentioned above. This paper describes how these two aspects can be treated by allowing inhomogeneous states of polymer in a variational theory. To this end, we derive free energy functionals written in terms of field variables and seek saddle point solutions of them, which are called the *droplet* solutions, or instanton solutions.

Our current understanding of the thermodynamic folding barrier $F^{\ddagger}$ and the size of a critical folding nucleus in real proteins is still rudimentary and there are elements of controversy. Long ago, Bryngelson and Wolynes estimated a size of nucleus based on a capillarity picture yielding quite a large size.[3] Through mutation studies, Fersht *et al.* suggested that CI2 has *hot spots* which consist of a particular group of three amino acids which might be identified as a sort of folding nucleus.[4] It should be noted, however, that the experiments indicate many partially ordered residues accompany these three residues in acquiring structure at the bottleneck.[4–6] Combining lattice simulations with sequence database information, Shakhnovich *et al.*[7] concluded that the most conserved residues in the evolution process dominantly contribute to a specific folding nucleus, while Thirumalai and Guo argued, from their off-lattice simulation, that a mobile nucleus is quite large, and includes quite random hydrophobic contacts, although there are some preferred regions around flexible loop regions.[8]

Quantifying the other factor, τ, in the folding kinetics, is even harder and related to problems confronted in many studies of disordered systems. In a disordered collapsed globule, trap escape will be rate limiting at low temperature, and this trap escape time scale is largely determined by the typical barrier height that the protein needs to overcome for reconfiguration. For larger proteins, how the escape barrier grows with the size is interesting and controversial.[2,9,10] The barriers computed in the strict mean field limit of uniform global transitions are of order $\sim 0.1 N k_B T_K$ at the static transition T_K,[11] using parameters fit to the lattice model thermodynamics,[12] where N is the number of residues. This seems to be consistent with recent simulation results of the lattice model at low temperature.[9] Our calculations given here suggest that local inhomogeneous transition, which we call *entropic droplets*, can reduce the barrier height of reconfiguration for larger proteins, while the mean field arguments remain a good starting point for smaller proteins. Especially since folding simulations nowadays can only address rela-

tively short polymers, qualitative and quantitative analytical work for longer chains is highly desired.

We consider a standard interacting-beads Hamiltonian with a term explicitly representing the effect of the minimal frustration of the native structure of fast folding proteins,

$$H = k_B T A \sum_i (\mathbf{r}_{i+1} - \mathbf{r}_i)^2 + \tfrac{1}{2} \sum_{i \neq j} b_{ij} u(\mathbf{r}_i - \mathbf{r}_j) + \frac{c}{6} \sum_{i \neq j \neq k} u(\mathbf{r}_i - \mathbf{r}_j) u(\mathbf{r}_j - \mathbf{r}_k) + \epsilon_{\mathrm{Nat}} \sum_{(\mu\nu)}^{(\mathrm{N})} u(\mathbf{r}_\mu - \mathbf{r}_\nu)$$
$$= H_0(\{\mathbf{r}_{ij}\}) + H_1(\{\mathbf{r}_{ij}\}, b_{ij}, c) + H_{\overline{\mathrm{Go}}}(\{\mathbf{r}_{ij}\}). \quad (2)$$

Here $\mathbf{r}_i$ represents positions of Kuhn segments ($i = 1 \sim N$), $A = (2a^2)^{-1}$ where a is the Kuhn length, b_{ij} and c are the second and third virial coefficients, respectively, and $u(\mathbf{r}) = \exp(-\mathbf{r}^2/\sigma^2)$, where σ is the characteristic length of interactions. $\Sigma^{(\mathrm{N})}$ means that the sum is taken over only native pairs. The first term (H_0) describes the polymeric connectivity, the second and third terms (H_1) are virial type interactions, and the last term ($H_{\overline{\mathrm{Go}}}$) is similar to the one used by $\overline{\mathrm{Go}}$ *et al.*[13] and realizes the principle of minimal frustration;[1] the parameter $\epsilon_{\mathrm{Nat}} < 0$ controls the strength of this effect. Notice that this model does not have inhomogeneity for forming native contacts. For the latter, we can consider the term $\Sigma^{(\mathrm{N})}_{(\mu\nu)} \epsilon_{\mu\nu} u(\mathbf{r}_\mu - \mathbf{r}_\nu)$ instead of the $\overline{\mathrm{Go}}$ term. We also note that one caveat of the model is that polymers have additional entanglement constraints, i.e., the chain is uncrossable; this is not taken into account in the present study.

In Sec. II we study the activation barrier $F^\ddagger$ for the folding via a nonspecific folding nucleus route. Using the $\overline{\mathrm{Go}}$-type model, a free energy functional is derived and its saddle point solution, i.e., the droplet solution, is sought numerically to estimate the folding barriers. Since proteins are too small to be thought of as purely macroscopic matter, we must discuss the finite size effects on this folding nucleus. Section III addresses the reconfiguration rates τ near the glass transition temperature, where this has a highly nontrivial temperature dependence. Near, but above, the static glass transition temperature, the free energy landscape has multiple metastable minima of trapped states, and transitions among them determine reconfiguration rates in the folding reaction coordinate. Replica instanton calculations are developed to describe inhomogeneous states, which we call entropic droplets, allowing us to quantify the reconfiguration barrier. Results in the above two sections are combined to calculate the folding time based on Eq. (1) in Sec. IV. Conclusions are given in Sec. V.

II. A NONSPECIFIC CRITICAL FOLDING NUCLEUS

In this section we address the barrier for the folding via a nonspecific nucleus route as appropriate for the uniformly minimal frustrated model. The nonspecific nucleus route assumes that folding transition states correspond to formation of a certain number of native contacts without specifying which particular pairs, although requiring them to be relatively compact in space. This is in contrast to a specific nucleus route where formation of particular amino acid pairs is rate limiting. This might apply to the heterogeneously biased model mentioned above if the native contact energies are widely distributed. Obviously, these two routes are in some sense opposite limiting cases, and real proteins may adopt some routes in between these two cases. In case a very small critical nucleus allows folding, heterogeneity effects will be larger and a specific nucleus may be more advantageous, while if the nucleus is large, it becomes, of necessity, more nonspecific.

A. A mean field approach

For a well designed protein, the folding transition temperature T_F is significantly higher than the static glass transition temperature T_K. Thus, at a temperature below but near T_F, we can as a first approximation neglect the ruggedness of the free energy landscape. Thus, we consider here an unfrustrated model where $b_{ij} = b_0$ in the Hamiltonian Eq. (2).

For this model the critical folding nucleus is an inhomogeneous thermodynamic state where a part of protein has native contacts locally, but the rest is unfolded. To describe this, we introduce two field variables, the monomer density $\hat{\rho}$ and the native monomer density $\hat{\rho}_N$,

$$\hat{\rho}(\mathbf{r}) = \sum_i \delta(\mathbf{r} - \mathbf{r}_i), \quad (3)$$

$$\hat{\rho}_N(\mathbf{r}) = v \sum_i \delta(\mathbf{r} - \mathbf{r}_i)\, \delta(\mathbf{r}_i - \mathbf{r}_i^{(\mathrm{N})}), \quad (4)$$

where $\mathbf{r}_i^{(\mathrm{N})}$ is monomers' positions in the native state and $v^{1/3}$ defines the resolution of length scale, i.e., $\delta(\mathbf{0}) = v^{-1}$. The virial interaction terms H_1 can be written in terms of monomer density as

$$\hat{H}_1(\hat{\rho}_1(\mathbf{r}), b_0, c) \equiv H_1 = \frac{b_0}{2} \int d\mathbf{r}_1\, d\mathbf{r}_2\, \hat{\rho}(\mathbf{r}_1)\hat{\rho}(\mathbf{r}_2) u(\mathbf{r}_1 - \mathbf{r}_2) + \frac{c}{6} \int d\mathbf{r}_1\, d\mathbf{r}_2\, d\mathbf{r}_3\, \hat{\rho}(\mathbf{r}_1)\hat{\rho}(\mathbf{r}_2)\hat{\rho}(\mathbf{r}_3) \times u(\mathbf{r}_1 - \mathbf{r}_2) u(\mathbf{r}_2 - \mathbf{r}_3), \quad (5)$$

where we dropped small contributions which correspond to $i = j$ and $j = k$ terms in the summation of the original Hamiltonian. Since most of the native contacts are made only when two monomers are at the native positions, we can approximately write the $H_{\overline{\mathrm{Go}}}$ term in terms of the native monomer density,

$$\hat{H}_{\overline{\mathrm{Go}}}(\hat{\rho}_N(\mathbf{r})) \equiv H_{\overline{\mathrm{Go}}} = \frac{\epsilon_{\mathrm{Nat}}}{2} \int d\mathbf{r}_1\, d\mathbf{r}_2\, \hat{\rho}_N(\mathbf{r}_1)\hat{\rho}_N(\mathbf{r}_2) u(\mathbf{r}_1 - \mathbf{r}_2). \quad (6)$$

We express the canonical partition function in functional integral form

$$Z=\int \mathscr{D}\mathbf{r}_i \exp(-\beta H)$$
$$=\int \mathscr{D}\rho(\mathbf{r})\mathscr{D}\rho_N(\mathbf{r}) \times\exp[-\beta U(\rho(\mathbf{r})\rho_N(\mathbf{r}))+S(\rho(\mathbf{r})\rho_N(\mathbf{r}))/k_B], \quad (7)$$

where $\mathscr{D}\mathbf{r}_i\equiv\Pi_i d\mathbf{r}_i\ \delta(\Sigma\mathbf{r}_i)$ and U is the internal energy term for a given ρ and ρ_N,

$$U(\rho(\mathbf{r}),\rho_N(\mathbf{r}))=\hat{H}_1(\rho(\mathbf{r}),b_0,c)+\hat{H}_{\overline{\mathrm{Go}}}(\rho_N(\mathbf{r})), \quad (8)$$

and S is the chain conformational entropy term under the constraint of given ρ and ρ_N,

$$S(\rho(\mathbf{r}),\rho_N(\mathbf{r}))/k_B=\ln\left\{\int \mathscr{D}\mathbf{r}_i e^{-A\Sigma(\mathbf{r}_{i+1}-\mathbf{r}_i)^2} \times\delta(\hat{\rho}(\mathbf{r})-\rho(\mathbf{r}))\,\delta(\hat{\rho}_N(\mathbf{r})-\rho_N(\mathbf{r}))\right\}. \quad (9)$$

In real proteins, there is another contribution to the entropy. Namely, in each well-defined conformation, the chain still has some vibrational freedom to fluctuate, which leads to a vibrational entropy contribution. The latter does not exhibit any peculiar behavior and will be ignored here.

Before addressing the inhomogeneous situation, we first consider homogeneous solutions. We first employ the so-called volume approximation restricting the density to be given as $\rho(\mathbf{r})=\rho$ inside protein and $=0$ otherwise. In the same way, we also limit the variation of ρ_N to the form $\rho_N(\mathbf{r})=\rho_N\leqslant\rho$ inside protein and $=0$ otherwise. The internal energy terms are simply calculated as

$$U(\rho,\rho_N)=\frac{b_0}{2}N\rho\nu+\frac{c}{6}N(\rho\nu)^2+\epsilon_{\mathrm{Nat}}\frac{V\rho_N^2\nu}{2}, \quad (10)$$

where $\nu=(\pi\sigma^2)^{3/2}$ represents the volume that each bead can make interaction. The chain entropy is harder to estimate, especially in the collapsed phases in which we are interested. We present a simple estimate for the entropy under the two constraints, one for the monomer density, the other for the native monomer density. It is known that the entropy loss due to compaction is small and nonextensive,[14,15] and so the first constraint needs to be taken into account only very simply. To this end, we introduce a weak external potential $k_BTB\Sigma\mathbf{r}_i^2$ which is *conjugate* to the density so that we can control the monomer density by changing the external potential. We connect the radius of gyration $R_g\equiv\sqrt{\Sigma_i\langle\mathbf{r}_i^2\rangle/N}$ with the density by $N=4\pi R_g^3\rho/3$. Since R_g is a function of B, we obtain the relation between B and ρ. For the constraint on the native density, corresponding to the volume approximation used above, we replace $\hat{\rho}_N(\mathbf{r})$ with its space-averaged value $\hat{\rho}_N(\mathbf{r})\to\overline{\rho_N}\equiv V^{-1}\int d\mathbf{r}\hat{\rho}_N(\mathbf{r})$ inside protein and $=0$ otherwise. With these simplifications, we can write the entropy term as

$$e^{S(\rho,\rho_N)/k_B}=\int\frac{d\lambda}{2\pi i}\int\mathscr{D}\mathbf{r}_i\exp\left[-A\sum(\mathbf{r}_{i+1}-\mathbf{r}_i)^2 -B\sum_i\mathbf{r}_i^2-\lambda(\overline{\rho_N}-\rho_N)\right]$$
$$=\int\frac{d\lambda}{2\pi i}\int\mathscr{D}\mathbf{r}_i\exp[-\beta H_S(\mathbf{r}_i,\lambda)]$$
$$=\int\frac{d\lambda}{2\pi i}\exp[S(\lambda)], \quad (11)$$

where the second and third lines only define H_S and $S(\lambda)$, respectively. The stationary condition for the integration over λ directly leads to $\langle\overline{\rho_N(\mathbf{r}_i)}\rangle=\rho_N$ inside the protein, $=0$ otherwise. Now, we employ the Gibbs–Bogoliubov variational method for the *Hamiltonian* H_S to estimate $S(\lambda)$. The reference Hamiltonian we use is

$$\beta H_{\mathrm{ref}}(C)=A\sum(\mathbf{r}_{i+1}-\mathbf{r}_i)^2+B\sum\mathbf{r}_i^2+C\sum(\mathbf{r}_i-\mathbf{r}_i^{(\mathrm{N})})^2, \quad (12)$$

where C measures the distance from native structure and is essentially correlated with the variable ρ_N. With this reference Hamiltonian, the standard formula gives

$$-S(\lambda)=-\ln Z_{\mathrm{ref}}+\beta\langle H_S-H_{\mathrm{ref}}\rangle_{\mathrm{ref}}, \quad (13)$$

where $\langle\ \rangle_{\mathrm{ref}}$ means the expectation value about the reference Hamiltonian and Z_{ref} is the partition function of the reference Hamiltonian.

The basic calculation using this reference Hamiltonian needed here has already been presented in Sasai and Wolynes,[15] and Takada and Wolynes.[12] We simply borrow their results yielding in the native phase ($C\gg A$),

$$-S(\lambda)=\tfrac{3}{2}N\ln\frac{C}{A}+\lambda(\langle\overline{\rho_N}\rangle_{\mathrm{ref}}-\rho_N)=\tfrac{3}{2}N\ln\frac{C^*(\rho_N)}{A}, \quad (14)$$

and $\rho_N\sim\rho v(C/\pi)^{3/2}\leqslant\rho$. Thus, the entropy term can be written in terms of the native monomer density

$$S(\rho,\rho_N)/k_B=N\ln\left(\frac{\rho_N}{\rho}\gamma+1\right), \quad (15)$$

where $\gamma=(\pi/A)^{3/2}/v$. For practical purposes, we have used a simple interpolation so that the entropy behaves appropriately even in the unfolded phase, i.e., $S(\rho,\rho_N=0)=0$. (Note that we are measuring entropy relative to the random coil state, namely this is the entropy loss due to confinement.[12,15]) Finally, the total free energy is given by the formula,

$$F(\rho,\rho_N)=U(\rho,\rho_N)-TS(\rho,\rho_N), \quad (16)$$

which gives the free energy in homogeneous states. We depict free energies per monomer as a function of ρ_N for a few temperatures in Fig. 1. Hereafter, for illustration, we use a single parameter choice: $\gamma=5$, $\sigma=1$, and $\rho=1$ ($k_B=1$ so that temperature is measured in the unit of energy). γ is the number of possible conformation per bead, which is 5 for a cubic lattice model and a reasonable estimate for a flexible

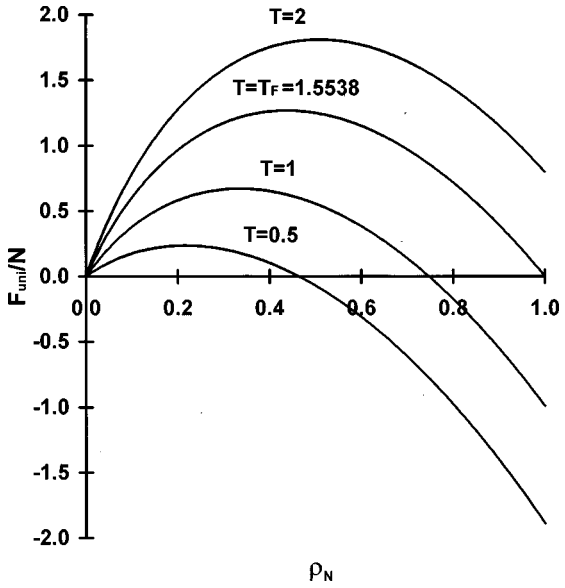

FIG. 1. Free energy (bulk terms only) as a function of native density ρ_N for several temperatures. Parameters used are $\rho=1$, $\gamma=5$, $\sigma=1$, and $\epsilon_{\mathrm{Nat}}=-1$.

chain, too.[14] $\sigma=1$ leads to $\rho\nu=5.57$. Remembering that $\rho\nu$ is the number of interacting neighbors per bead, we see 5.57 is close to the coordination number of cubic lattice model protein. In Fig. 1, as is usual, the folded state $\rho_N=\rho$ is only metastable at very high temperature, becomes equal in energy to the unfolded phase at the folding transition temperature T_F, and is the global minimum at $T<T_F$. The barrier height for a homogeneous transition is simply N times the value of the free energy at the barrier (denoted by $\rho_N^{\ddagger}$).

B. Folding nucleus: Energetic surface tension

To calculate the size of the critical folding nucleus, we need to compute the surface tension. There are two terms that contribute to the surface tension, one energetic and the other entropic. In this subsection, we deal with the energetic surface effect, while the entropic one is calculated in the next subsection. To this end, in estimating the interaction energy, we consider the inhomogeneous case where ρ is still constant, but ρ_N is a slowly varying function in space. The so-called gradient expansion yields a surface tension term;[16] we first change integration variables in H_{Go} terms to $\mathbf{r}\equiv(\mathbf{r}_1+\mathbf{r}_2)/2$ and $\Delta\mathbf{r}\equiv\mathbf{r}_1-\mathbf{r}_2$ and expand the integrand in $\Delta\mathbf{r}$ up to the second order. This gives

$$\hat{H}_{\mathrm{Go}}=\frac{\epsilon_{\mathrm{NAT}}}{2}\,\nu\int d\mathbf{r}\left[\rho_N(\mathbf{r})^2-\frac{\sigma^2}{4}\,(\nabla\rho_N(\mathbf{r}))^2\right], \tag{17}$$

where the term including ∇ yields a surface tension. Thus the total free energy functional becomes

$$F[\rho_N(\mathbf{r})]=F_{\mathrm{globule}}+\int d\mathbf{r}\left\{\frac{\epsilon_{\mathrm{Nat}}}{2}\,\nu\left[\rho_N(\mathbf{r})^2-\frac{\sigma^2}{4}\,(\nabla\rho_N(\mathbf{r}))^2\right]+k_BT\rho\,\ln\left(\frac{\rho_N}{\rho}\,\gamma+1\right)\right\}, \tag{18}$$

for which we seek saddle solutions. There are two trivial solutions. One corresponds to remaining at $\rho_N=0$ and the other at $\rho_N=\rho$ forever. These two homogeneous solutions correspond to the unfolded phase and the folded phase, respectively.

We next consider a nontrivial saddle point solution of the free energy functional, in which a portion of the protein is folded while the rest is unfolded with a finite domain wall between the two portions. Just as for other first order transitions, this represents a critical folding nucleus. To find it, we utilize the customary analogy of the variational problem to classical mechanics.[17] Setting $M\equiv|\epsilon_{\mathrm{Nat}}|\nu\sigma^2/4$ and the homogeneous free energy density $f_{\mathrm{homo}}=\epsilon_{\mathrm{Nat}}\nu\rho_N^2/2+k_BT\rho\,\ln(\rho_N\gamma/\rho+1)$, we realize that the saddle condition becomes

$$\delta\int d\mathbf{r}[M(\nabla\rho_N)^2/2+f_{\mathrm{homo}}(\rho_N)]=0. \tag{19}$$

Therefore, if we assume a plane wall, the saddle equation for the perpendicular direction to the wall (we denote it z) can be viewed as Newton equations for a particle where the particle's *position, time, mass*, and *potential* correspond to ρ_N, z, M, and the inverse free energy $-f_{\mathrm{homo}}$, respectively. More realistically, the surface can be assumed to be spherical rather than plane minimizing the surface energy cost. In that case, the equation of motion becomes

$$M\,\frac{d^2\rho_N}{dr^2}=\frac{df_{\mathrm{homo}}}{d\rho_N}-M\,\frac{2}{r}\,\frac{d\rho_N}{dr}, \tag{20}$$

where the last term, coming from curvature of the surface, corresponds to *friction* in classical mechanics. This picture helps us find solutions. The nontrivial solution corresponding to the critical nucleus is a *trajectory* that stays at the folded phase $\rho_N=\rho$ from *time* $r=0$, after a while, goes downhill to $\rho_N=\rho_N^{\ddagger}$ at *time* $r^{\ddagger}$, then finally proceeds uphill, and stops at the unfolded phase $\rho_N=0$. We note that below T_F, the *potential* $-f_{\mathrm{homo}}$ is larger at the folded phase than at the unfolded phase, and that the *friction* strength decreases monotonically from infinity to zero in increasing *time* r. Thus, we always find one and only one solution (characterized by $r^{\ddagger}$) where the free energy difference between folded and unfolded phases precisely compensates the energy loss during a travel. Figure 2 depicts the critical radius of the nucleus as a function of temperature. The folding nucleus grows as temperature increases until T_F, where the radius diverges to infinity. The free energy barrier, the energy difference between the unfolded state and the nucleus state, is plotted in Fig. 3(a). As expected from the size of the nuclei, the barrier increases very sharply as temperature increases up to T_F. The shape and the breadth of the domain wall is plotted in Fig. 4, where we find that the breadth of the wall is about 1.5σ, rather thin. We note that we are implicitly thinking of an infinitely long chain so far, while real proteins with finite sizes have a cutoff. This will be discussed below.

Since the domain wall obtained from these calculations is thin compared with the size of larger proteins (but not necessarily so for smaller ones), we can neglect the breadth

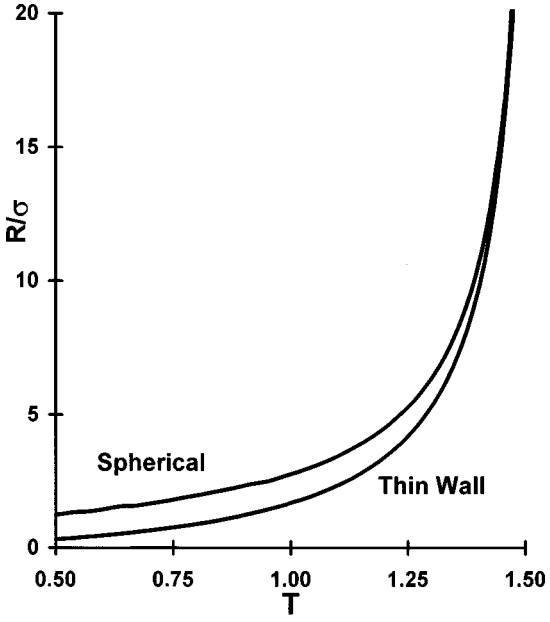

FIG. 2. Radius of folding nucleus as a function of temperature. Solid (dashed) curve represents the result from the spherical droplet (the thin wall approximation). Parameters used are the same as Fig. 1.

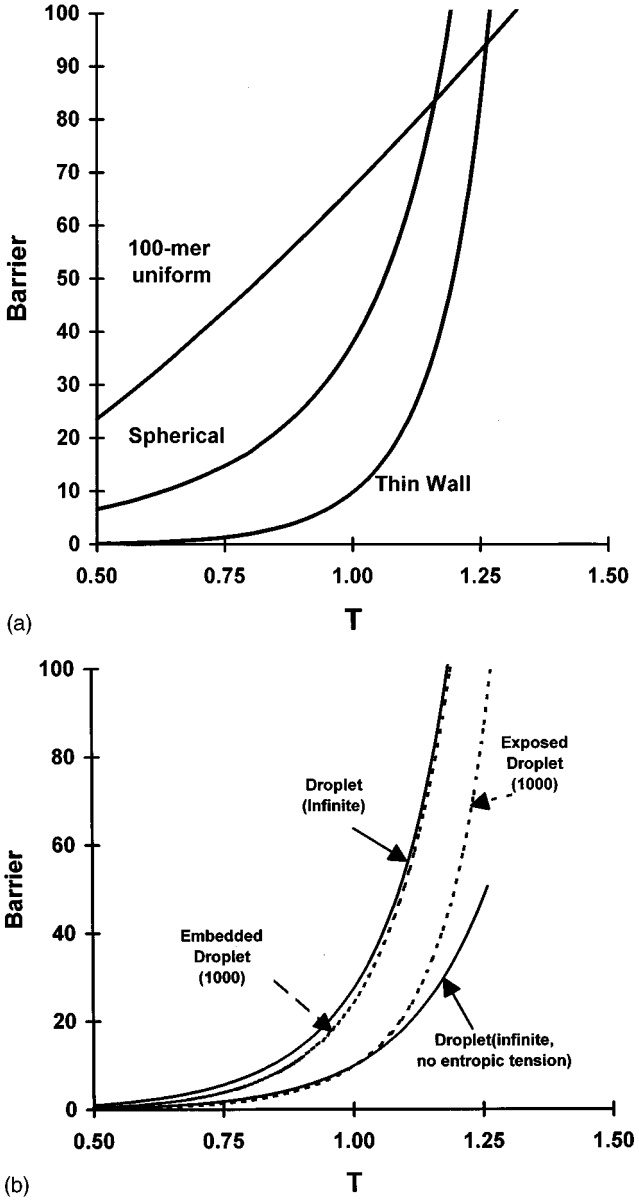

FIG. 3. Barriers for folding nucleus as a function of temperature. (a) The case where entropic surface tension is not taken into account. Each curve is for 1) the spherical droplet, 2) the droplet by the thin approximation, 3) the 100-mer uniform transition, and 4) the edge droplet in finite size proteins (100 mer and 1000 mer, see text for more details). We note that the barrier for the uniform transition in the 1000 mer is ten times higher than that in the 100 mer, and is far out of the range of the figure. (b) The case where entropic surface tension is taken into account. The thin wall approximation is always employed here. 1) droplet of infinite system (solid curve), 2) embedded droplet for a 1000 mer (dotted curve), 3) exposed droplet for a 1000 mer (see text for more details, dotted curve in the figure), and 4) (for comparison) droplet of infinite system (solid curve) when the entropic surface tension is *not* included. Parameters used are the same as Fig. 1.

and therefore the curvature of the domain wall for larger proteins. This is called the thin wall approximation.[17] Within this approximation, we can solve the nondissipative Newton equation for a plane wall obtaining the surface tension $\Sigma_H = M\int dz(d\rho_N/dz)^2$, where z is a coordinate running perpendicular to the wall. An approximate free energy of the nucleus with the radius R_N can be written as

$$F_{\text{thin}}(R_N) = 4\pi R_N^2 \Sigma_H - (4\pi/3) R_N^3 \Delta f, \tag{21}$$

where Δf is the difference in free energy density between the unfolded and folded states. The critical radius $R_{N,c} = 2\Sigma_H/\Delta f$ and the free energy barrier $F^{\ddagger} = 16\pi\Sigma_H^3/3\Delta f^2$, estimated by the thin wall approximation, are plotted in Figs. 2 and 3(a), respectively. As is clear from the *friction* term, this approximation becomes accurate for a large nucleus. We should note that, quantitatively speaking, the gradient expansion approach we take here may not be so accurate since the domain wall is quite thin; for higher accuracy, we need more involved estimates of the wall structure.[18]

C. Entropy contribution to the surface tension

There can be another surface of source tensions, the entropic surface tension.[19] In general, the surface of a nucleus divides a chain into many folded segments in the nucleus and globule segments outside the nucleus. Since chain segments in the nucleus are strongly bound to a given location and fluctuate only around their native positions, their contribution to the conformational entropy is extensive to a good approximation. On the other hand, each segment of the rest of the chain which is in the globule state fluctuates globally with both ends fixed, which leads to a logarithmic entropy term in the length of the segment as in the random coil phase. This means that the sum of the entropies over the unfolded segments is not the same as that of one chain whose length is equal to the sum of these segments' lengths. Namely, pinning a long chain into many shorter segments loses some entropy and so costs free energy. We call this difference the *entropic surface tension*, because it is the nonextensive part of the free energy. The origin of the entropic surface tension is quite different from ordinary surface tension.

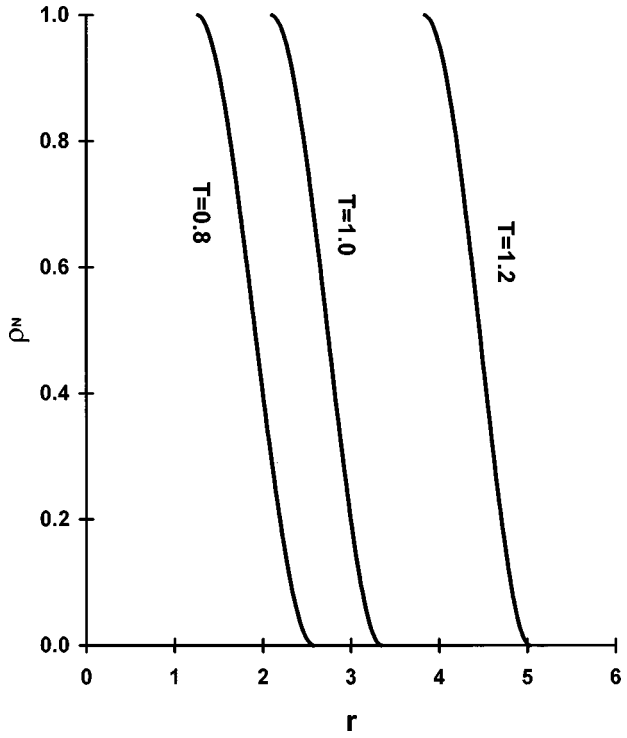

FIG. 4. The shape of the domain wall of folding nucleus at temperature $T/|\epsilon_{\rm Nat}|=0.8$, 1.0, and 1.2. Parameters used are the same as Fig. 1.

Now, we describe the above mentioned idea more explicitly. First, we compute the conformational entropy of a globule state where each end point is fixed within a length scale of c. Denoting the positions of both ends as $\mathbf{r}_0$ and $\mathbf{r}_{M+1}$, we can write the entropy as

$$S/k_B=\ln\int\prod_{i=1}^{M}d\mathbf{r}_i\,\exp\Bigg[-A\sum_{i=1}^{M-1}(\mathbf{r}_{i+1}-\mathbf{r}_i)^2 - C_N(\mathbf{r}_1-\mathbf{r}_0)^2-C_N(\mathbf{r}_{M+1}-\mathbf{r}_M)^2\Bigg], \tag{22}$$

where M is the length of a segment and $C_N=(2c^2)^{-1}$. In our case, C_N is the value of $C=\pi v^{-2/3}$ in the nucleus part. Since we know *a posteriori* that short segments are dominant, we approximately set $\mathbf{r}_0=\mathbf{r}_{M+1}=\mathbf{0}$. Then a straightforward calculation leads to

$$S/k_B=\frac{3}{2}M\,\ln\frac{\pi}{A}-\frac{3}{2}\ln\left[\left(\frac{C_N}{A}\right)^2 M\right], \tag{23}$$

where the first term is extensive and is the same as that of free chain, while the second term, which is due to the fixed boundary, is indeed logarithmic in the length of the segment and will be used as the entropic surface tension below.

We next estimate the average number of occurrences of a segment with length M. The probability that the monomer i and $i+M$ are found within the distance $L\sim 1/\sqrt{C_N}$ is

$$P_M=\left(\frac{A}{\pi M}\right)^{3/2}L^3.$$

Assuming that this contact is distributed uniformly in space, we find the probability density of contacts with loop length M is $P_M(N-M)/V$, where V is the total volume of the protein. When some contacts are formed at the surface of the nucleus, about half of them make loops outside the nucleus. Collecting all these factors together, we write the nonextensive part of free energy coming from entropy as

$$\Sigma_S=\tfrac{3}{4}k_BT\sigma_{\rm wall}\rho\sum_M\left(\frac{N-M}{N}\right)\times\left(\frac{A}{C_N\pi M}\right)^{3/2}\ln\left[\left(\frac{C_N}{A}\right)^2 M\right], \tag{24}$$

where $\sigma_{\rm wall}$ is the breadth of the domain wall of the nucleus. In the summation, small M terms dominate because of the $M^{-3/2}$ dependence, although the convergence is quite slow and long loops are not completely negligible.

With the same parameters as above, we computed this entropic surface tension and estimated the modified barrier of critical folding nucleus within the thin wall approximation. Here we kept the breadth of the wall the same as before and used it for the estimate of Σ_S. Figure 3(b) depicts the free energy barriers for the case where the entropic surface tension is taken into account as well as those for which the case entropic effect is ignored. The entropic contribution to the tension is about 30%–40% of the energetic one in the temperature range shown here. Thus, the barrier increases somewhat due to the chain entropy effect. The entropic surface tension seems to be non-negligible, though it is still quite a bit smaller than the energetic contribution.

D. Finite size effects

So far, the droplet calculation has been done for an infinite size system, or at least a sufficiently large system. Since proteins are too small to be thought of as completely macroscopic systems, we consider some finite size effects. First of all, the transition temperature estimated only by bulk terms, such as that given above, needs to be corrected due to a non-negligible effect of the surface tension.[20] Namely, the size dependent folding temperature $T_F(N)$ can be defined by the condition that the native state has the same free energy as the unfolded state. Within the thin wall approximation, this becomes

$$F_{\rm thin}(R_{\rm tot})=4\pi R_{\rm tot}^2\Sigma_H-(4\pi/3)R_{\rm tot}^3\Delta f=F_{\rm thin}(0),$$

which leads to $R_{\rm tot}=3\Sigma_H(T_F)/\Delta f(T_F)$. Note that the entropic surface tension is zero on the surface of proteins because it arises when the chain is divided by the surface. Using the same parameters as above, we get $T_F(100\ \text{mer})=1.06|\epsilon_{\rm Nat}|$, $T_F(1000\ \text{mer})=1.26|\epsilon_{\rm Nat}|$ in contrast to the bulk value $T_F=T_F(\infty)=1.554|\epsilon_{\rm Nat}|$. This is quite a large effect. Because of the smallness of proteins, the surface forces play a significant role even for static properties such as the folding temperature.

Another question arising from the finiteness of proteins is whether the nucleus is buried in the protein or located near the surface. This is a rather subtle question depending on

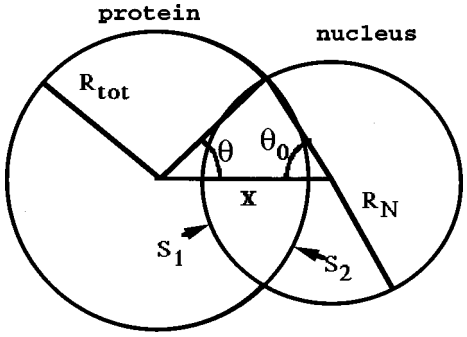

FIG. 5. Cross section of a droplet in a finite spherical protein.

detailed surface tension calculations. For simplicity, we restrict our variational search space by fixing both the shape of the protein and of the folding nucleus as spheres, taking the nucleus as either completely embedded in the protein or exposed to the surface of the protein. In the latter case, the nucleus is approximately the overlap region of two spheres. Looking at a section of our model, Fig. 5, we note that there are two kinds of surfaces of the droplet, of which the surface tensions would generally be different from each other: the surface of the droplet inside the protein, S_1, and that exposed to the solvent, S_2. On S_2 the entropic surface tension is zero, as is mentioned above. Also, since monomers near the surface of the protein can make contacts with fewer monomers than inside the protein, we should have some energetic surface tension on S_2. But, the energetic surface tension on S_2 would be affected by the monomer density ρ, which is also smaller at the surface than inside the protein. Thus, the energetic surface tension on S_2 might be smaller than that on S_1, although we have not estimated how different they are. Here, we study two extreme limits: the case where both energetic surface tensions are the same, and the case where the energetic surface tension on S_2 is negligible. Real proteins should fall in between the two cases.

First we assume the energetic surface tension is the same at both S_1 and S_2, while the entropic surface tension exists only at S_1. We computed surface areas S_1 at the surface S_1 and S_2 at the surface S_2, and the volume V of the nucleus as a function of the radius of the nucleus R_N and the offset distance x, which is the length between the center of the protein sphere and that of the nucleus (see Fig. 5). Detailed formulae are given in the Appendix. The barrier state is defined as a saddle point of $F=\Sigma_H(S_1+S_2)+\Sigma_S S_1-\Delta fV$ in the (R_N,x) plane. We find that the optimal location for x is a little bit larger than $R_{\rm tot}-R_N$, which corresponds to the situation that the nucleus sphere is largely embedded in the protein, but a tiny portion is exposed to the surface. For larger nuclei, the exposed portion increases. We plot the thermodynamic folding barrier obtained from this assumption in Fig. 3(b). (We call this an ''embedded'' nucleus.) Since the exposed portion is small, the barrier obtained from this assumption is almost identical to that of the infinite model. This set of internal residues or embedded nucleus resembles the structure deduced from protein engineering experiments on CI2.[4]

We can also take the second limit where we ignore both the energetic and entropic surface tension of the nucleus at S_2. Thus, the free energy is $F=(\Sigma_H+\Sigma_S)S_1-\Delta fV$. The barrier state always turns out to be located at $x\sim R_{\rm tot}$. That is, the nucleus is always centered at the surface of the protein. The folding barrier height is greatly diminished when this choice pertains, as is shown in Fig. 3(b) (we call this an ''exposed'' or turn nucleus). This nucleus resembles the type postulated originally by Scheraga[21] and apparently seen in the simulations of minimalist models by Thirumalai and Guo.[8] We should remind the reader that this is a consequence of our assumption that the surface tension at S_2 is negligible.

III. ENTROPIC DROPLETS: LOCAL TRANSITIONS BETWEEN MISFOLDED STATES

In this section, we address the other important factor involved in folding kinetics, namely, the reconfiguration time τ. At a relatively high temperature, this is only weakly temperature dependent and is of the order of a microscopic time scale for chain motion, so that the rate is largely determined by the folding barrier discussed already. As temperature decreases to the static glass transition temperature, the reconfigurations occur through thermally activated events, allowing transition between many metastable states on the rugged energy landscape. Since the landscape gets more and more rugged upon cooling, τ increases up to a mesoscopic scale. Here, we describe the barrier between these metastable states via small localized fluctuations, which we call *entropic droplets*.

For simplicity, we consider a random heteropolymer where the $\overline{Go}$-term $H_{\overline{\rm Go}}$ is set to zero and the second virial coefficients b_{ij} are Gaussian random variables with distribution, $P(b_{ij})=(2\pi b^2)^{-1/2}\exp[-(b_{ij}-b_0)^2/2b^2]$, and focus on the temperature range near the glass transition. The droplet we consider is a small globular region of the polymer that may take on many configurations, local in space but not necessarily in sequence, buried in a remaining frozen glassy portion. We utilize replica formalism and derive a Landau-like free energy functional in terms of the Debye–Waller factor for a residue that plays the role of an Edwards–Anderson order parameter which is taken as spatially varying. By seeking a saddle solution of this functional, we can compute the reconfiguration barrier and thus the time scale for trap escape from metastable minima. A brief report of this calculation is found in Ref. 22.

A. Physical background

Quantifying escape from configurational traps on a rugged free energy landscape is important for understanding the dynamics of spin glasses,[23] structural glasses[24] and folded proteins,[25] and for protein folding.[1] A first step toward understanding barriers is to appreciate the organization of the stable minima.[26] This has only been carried out completely for infinite range spin glasses. That organizational structure inspires many of the dynamical theories[1,12,15,27,28] of protein folding. Barriers in mean field spin glasses scale with the system size, but the finite range of interactions allows escape

from traps through localized reconfigurations with finite barriers in the thermodynamic limit. The Vogel–Fulcher law for viscosity of structural glasses has been explained through such a mechanism.[29] Various mean field theories of structural glasses resemble those for spin glasses lacking reflection symmetry. In strict mean field theory these models undergo a dynamical transition at a temperature T_A (''A'' means activated, see below), where a macroscopic number of frozen free energy minima appear, and a static transition at T_K, the Kauzmann temperature, where the configurational entropy of the minima disappears ($T_A > T_K$). Kirkpatrick and Wolynes (KW) pointed out that that individual free energy minima between T_A and T_K will be inherently unstable for short range interaction models because of entropic droplets: the extensive configurational entropy provides a driving force for a localized region in a local minimum to reconfigure and escape the trap. Thus, thermally activated events control the dynamics in this temperature range. Their analysis gave a modified Vogel–Fulcher law while a later scaling picture incorporating entropic droplets gave precisely the usual form used empirically.[30] Parisi has presented a novel instanton argument in replica space yielding the original KW form.[31] Here, we use replica instanton calculations to quantify reconfiguration barriers for the random heteropolymer.

B. The replica formalism for homogeneous states

We only briefly overview the replica formalism used here since it is largely the same as that in Takada and Wolynes[12] except for one significant difference, namely, that our order parameters are allowed to vary slowly in space to describe droplets in the following section. The free energy $F_{\rm av}$ averaged over quenched randomness is calculated using the standard replica formalism,[26]

$$-\beta F_{\rm av} = [\ln Z]_{\rm av} = \lim_{n\to 0} \frac{[Z^n]_{\rm av} - 1}{n}, \tag{25}$$

where n is the number of replicas. In the same spirit as the previous section, we introduce an overlap order parameter function $\hat{Q}_{\alpha\beta}$,

$$\hat{Q}_{\alpha\beta}(\mathbf{r}_1,\mathbf{r}_2) = \sum_i \delta(\mathbf{r}_1 - \mathbf{r}_i^\alpha)\,\delta(\mathbf{r}_2 - \mathbf{r}_i^\beta), \tag{26}$$

where α and β are replica indices. The monomer density in replica space can be defined using $\hat{Q}$ by

$$\hat{\rho}_\alpha(\mathbf{r}_1) = \int \hat{Q}_{\alpha\beta}(\mathbf{r}_1,\mathbf{r}_2)\,d\mathbf{r}_2 = \sum_i \delta(\mathbf{r}_1 - \mathbf{r}_i^\alpha). \tag{27}$$

In computing $[Z^n]$, we first average over randomness, obtaining an effective Hamiltonian $\mathscr{H}_{\rm eff}$ in the replica space,

$$[Z^n]_{\rm av} = \int \mathscr{D}\mathbf{r}_i^\alpha e^{-\beta \mathscr{H}_{\rm eff}}, \tag{28}$$

where $\mathscr{D}\mathbf{r}_i^\alpha \equiv \Pi_{i,\alpha} d\mathbf{r}_i^\alpha\ \Pi_\alpha \delta(\Sigma_i \mathbf{r}_i^\alpha)$, and the effective Hamiltonian is

$$\mathscr{H}_{\rm eff} = \sum_\alpha H_0(\{\mathbf{r}_i^\alpha\}) + \sum_\alpha \hat{H}_1\left(\hat{\rho}_\alpha(\mathbf{r}), b_0 - \frac{\beta b^2}{2}, c\right) + \hat{\mathscr{H}}_2(\hat{Q}_{\alpha\beta}(\mathbf{r}_1,\mathbf{r}_2)). \tag{29}$$

Here, H_0 and $\hat{H}_1$ are defined in Eqs. (2) and (5), and the inter-replica interaction part $\mathscr{H}_2$, responsible for breaking ergodicity, can be written in terms of the overlap order parameters as

$$\hat{\mathscr{H}}_2 = -\frac{\beta b^2}{4} \int d\mathbf{r}_1\, d\mathbf{r}_2\, d\mathbf{r}_3\, d\mathbf{r}_4 \times \left[\sum_{\alpha\neq\beta} \hat{Q}_{\alpha\beta}(\mathbf{r}_1,\mathbf{r}_2)\hat{Q}_{\alpha\beta}(\mathbf{r}_3,\mathbf{r}_4)\right] \times e^{-[(\mathbf{r}_1-\mathbf{r}_3)^2 + (\mathbf{r}_2-\mathbf{r}_4)^2]/\sigma^2}. \tag{30}$$

The partition function can be expressed in functional integral form as in the previous section,

$$[Z^n]_{\rm av} = \int \mathscr{D}Q_{\alpha\beta}(\mathbf{r}_1,\mathbf{r}_2) \exp\{-\beta \mathscr{U}[Q_{\alpha\beta}(\mathbf{r}_1,\mathbf{r}_2)] + \mathscr{S}[Q_{\alpha\beta}(\mathbf{r}_1,\mathbf{r}_2)]/k_B\}, \tag{31}$$

where the internal energy is

$$\mathscr{U}[Q_{\alpha\beta}(\mathbf{r}_1,\mathbf{r}_2)] = \sum_\alpha \hat{H}_1\left(\rho_\alpha(\mathbf{r}), b_0 - \frac{\beta b^2}{2}, c\right) + \hat{\mathscr{H}}_2(Q_{\alpha\beta}(\mathbf{r}_1,\mathbf{r}_2)), \tag{32}$$

and the chain conformational entropy is

$$\begin{aligned} e^{\mathscr{S}[Q_{\alpha\beta}(\mathbf{r}_1,\mathbf{r}_2)]/k_B} &= \int \mathscr{D}\mathbf{r}_i^\alpha e^{-A\sum_{i\alpha} (\mathbf{r}_{i+1}^\alpha - \mathbf{r}_i^\alpha)^2} \times \prod \delta(\hat{Q}_{\alpha\beta}(\mathbf{r}_1,\mathbf{r}_2) - Q_{\alpha\beta}(\mathbf{r}_1,\mathbf{r}_2)) \\ &= \int \prod \frac{d\lambda_{\alpha\beta}}{2\pi i} \int \mathscr{D}\mathbf{r}_i^\alpha \exp[-\beta \mathscr{H}_S(\mathbf{r}_i^\alpha, \lambda_{\alpha\beta})]. \end{aligned} \tag{33}$$

Here, the bottom expression means that the δ function in the previous line is represented in integral form and the resulting exponent is written as $\mathscr{H}_S$.

The variational approach extended into replica space[12,15,32] can be used with a reference Hamiltonian $H_{\rm ref}$ to calculate an approximate $\mathscr{S}$,

$$-\mathscr{S}/k_B = -\ln \mathscr{Z}_{\rm ref} + \beta\langle \mathscr{H}_S - \mathscr{H}_{\rm ref}\rangle_{\rm ref}.$$

Here, $\mathscr{Z}_{\rm ref}$ is the partition function for $\mathscr{H}_{\rm ref}$, and $\langle\cdots\rangle_{\rm ref}$ means the average over $\mathscr{H}_{\rm ref}$. We use the same reference Hamiltonian as Takada and Wolynes[12] (with $C=0$),

$$\beta\mathscr{H}_{\rm ref}(D,m) = A\sum_{\alpha,i} (\mathbf{r}_{i+1}^\alpha - \mathbf{r}_i^\alpha)^2 + B\sum_{\alpha,i} (\mathbf{r}_i^\alpha)^2 + D\sum_{\alpha\neq\beta,i} d_{\alpha\beta}(\mathbf{r}_i^\alpha - \mathbf{r}_i^\beta)^2, \tag{34}$$

where B measures the confinement to a globule as in the previous section, and D and $d_{\alpha\beta}$ are variational parameters specifying the vibrational freedom in a minimum and the replica symmetry breaking related to the configurational entropy, respectively. We assume $d_{\alpha\beta}$ has the same structure as mean field Potts spin glasses; n replicas are divided into n/m groups, each of which has size m, and the matrix element $d_{\alpha\beta}$ is 1 if α and β ($\alpha \neq \beta$) belong to the same group, and 0 otherwise. It is straightforward, though cumbersome, to obtain $\mathscr{S}_{\rm var}$ as a function of these parameters. As in Ref. 12, the *homogeneous* glassy state characterized by a large constant D (i.e., $D \gg A \gg B$) in the reference Hamiltonian yields an asymptotic high D expression for the entropy,

$$-\mathscr{S} = \frac{3}{2} N k_B n \, \frac{m-1}{m} \ln\left[\left(\frac{2}{A\sigma^2}\right) y + 1\right], \tag{35}$$

where y is a dimensionless Debye–Waller factor defined by $y = 2mD\sigma^2/2$. We used a simple interpolation to the $D=0$ limit, obtaining a globally appropriate expression.

The $\mathscr{H}_2$ term for homogeneous states can easily be obtained by inserting the mean value of $Q_{\alpha\beta}$ into Eq. (30). Namely,

$$\langle Q_{\alpha\beta}(\mathbf{r}_1, \mathbf{r}_2)\rangle_{\rm ref} = \rho_\alpha\left(\frac{\mathbf{r}_1+\mathbf{r}_2}{2}\right)\left(\frac{2mD}{2\pi}\right)^{3/2} e^{2mD(\mathbf{r}_1-\mathbf{r}_2)^2/2}, \tag{36}$$

when α and β are in the same group and $=0$ otherwise, and

$$\hat{\mathscr{H}}_2 = -\frac{\beta b^2}{4} 2^{-3/2} \nu n (m-1) \rho^2 \left(\frac{y}{y+1}\right)^{3/2}. \tag{37}$$

$\hat{H}_1$ is computed exactly in the same way as Sec. II as

$$\sum_\alpha \hat{H}_1 = n \, \frac{b_0}{2} N \rho \nu + n \, \frac{c}{6} N (\rho\nu)^2. \tag{38}$$

Collecting Eqs. (35), (37), and (38) yields the expression for homogeneous free energy,

$$F_{\rm av} = \frac{b_0}{2} N\rho\nu + \frac{c}{6} N(\rho\nu)^2 - \frac{\beta b^2}{4} 2^{-3/2} \nu (m-1) \times \rho^2 \left(\frac{y}{y+1}\right)^{3/2} + \tfrac{3}{2} N k_B T \, \frac{m-1}{m} \ln\left[\left(\frac{2}{A\sigma^2}\right) y + 1\right]. \tag{39}$$

The homogeneous solutions are essentially the same as in Ref. 12 for a δ function interaction model. Since ρ does not exhibit any peculiar behavior, we use the so-called volume approximation, where the monomer density $\rho_\alpha(\mathbf{r}) = \rho$ is taken inside the polymer, and zero otherwise. We first maximize $F_{\rm av}$ with respect to m for each y [denoting it as $m^*(y)$]. Figure 6 shows $f(m^*(y), y) \equiv F_{\rm av}/V$ for several temperatures, where V is the total volume of the polymer. In the high temperature limit, there is no saddle solution and only the globule state $y=0$ is stable. The dynamic glass transition takes place at the temperature T_A where a nonzero saddle solution $y>0$ appears. This describes a glassy trapped state. At temperatures below T_A, there are two minima in $f(y)$, one for the globule ($y=0$), which is thermodynamically equivalent to the sum over metastable minima, and the other for a particular metastable glassy minimum ($y = y_G > 0$). As temperature decreases, the free energies for the two solutions approach each other and become degenerate at the Kauzmann temperature T_K where the static transition occurs. As in spin glasses,[33] the uniform solution yields an estimate for the barriers between two lowest minima as the local maximum of $f(m^*(y), y)$, which we denote as occurring at $y^\ddagger$. Starting from zero at T_A, the uniform solution barrier height is extensive and grows as temperature decreases, and saturates around T_K.[12] T_A/T_K evaluated with typical parameters for flexible polymers [$(2a/\sigma)^2 = 4$, $\rho v = 1$] is about 1.4. Recently, T_A in essentially the same model has been estimated from a mode coupling theory, giving $T_A = 0.3b \pm 0.02b$,[34] which agrees quite well with the present value, 0.292 b.

C. Entropic droplets; inhomogeneous states

The globule state between T_A and T_K obtained by the ordinary replica theory represents a weighted sum of multiple local minima. Thus, the difference between the most probable free energy of a minimum and the globule free energy corresponds to the logarithm of the degeneracy of local minima, i.e., an extensive basin configurational entropy. For the *short range* infinite system between T_A and T_K, local minima are not separated by a thermodynamically large barrier but a finite one. KW argued that the free energy of an entropic droplet with a radius R is given by the conventional form $F \sim \Sigma R^2 - T s_c R^3$, where Σ is the surface tension and s_c is the configurational entropy density. Since s_c disappears at T_K, the critical size of the droplet diverges at T_K, where the static glass transition occurs.

An entropic droplet is described by an inhomogeneous situation where part of the polymer is trapped in a particular metastable state while another part can be in any minimum,

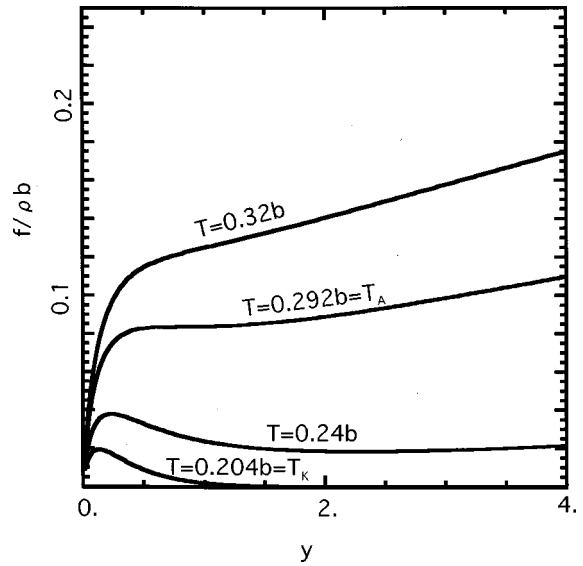

FIG. 6. Free energy density for the uniform solution as a function of $y = 2mD\sigma^2/2$ for several temperatures. The value of m is maximized for each y. Parameters used are $(2a/\sigma)^2 = 4$ and $\rho\nu = 1$ and temperatures are $T = 0.32b$, $0.292b \sim T_A$, $0.24b$, and $0.204b \sim T_K$.

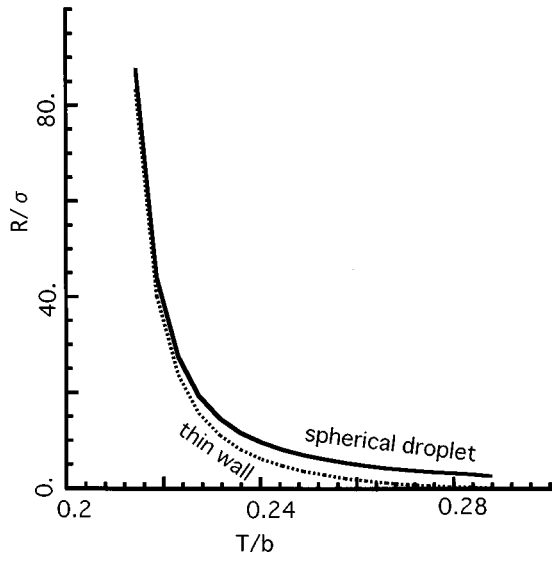

FIG. 7. Critical radii of droplet plotted with respect to T. The solid (dashed) curve represents the spherical droplet (that by the thin wall approximation). Parameters used are the same as Fig. 6.

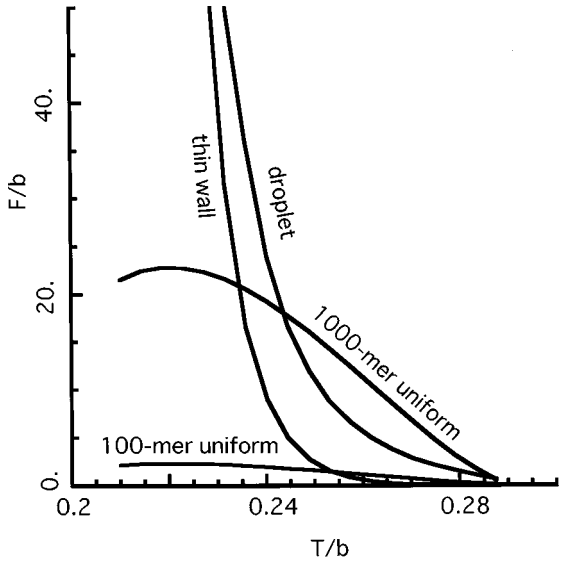

FIG. 8. Free energy barriers for droplets and uniform transitions with respect to T. Each curve is for 1) the droplet, 2) the droplet by the thin approximation, 3) the 100-mer uniform transition, and 4) that of 1000 mer. Parameters used are the same as Fig. 6.

i.e., in a globule state. The exterior of the droplet has large D describing the part trapped in a particular metastable region, while the interior with small D represents a region which can exist in multiple states. For explicitness, we shall assume that D varies slowly in the length scale of the interaction range σ.

To compute $\mathscr{H}_2$ for these inhomogeneous states, we use the expression for $Q_{\alpha\beta}$, Eq. (36), but take D to be a function of $(\mathbf{r}_1+\mathbf{r}_2)/2$ instead of a constant. Inserting this into Eq. (30), we can then transform integration variables, $\mathbf{R}_1 \equiv (\mathbf{r}_1+\mathbf{r}_2)/2$, $\Delta\mathbf{R}_1 \equiv \mathbf{r}_1-\mathbf{r}_2$, $\mathbf{R}_3 \equiv (\mathbf{r}_3+\mathbf{r}_4)/2$, and $\Delta\mathbf{R}_3 \equiv \mathbf{r}_3-\mathbf{r}_4$, so that we can integrate over $\Delta\mathbf{R}_1$ and $\Delta\mathbf{R}_3$. The resulting integrand is again transformed with $\mathbf{r} \equiv (\mathbf{R}_1+\mathbf{R}_3)/2$ and $\Delta\mathbf{r} \equiv \mathbf{R}_1-\mathbf{R}_3$. In the same way as used in the previous section for the thermodynamic folding barrier, we expand it with respect to $\Delta\mathbf{r}$ up to second order,[16] which gives the surface term as well as the bulk interaction term. With the use of the dimensionless Debye–Waller factor y, the free energy functional can be written in this approximation as $F[y(\mathbf{r})] = F_{\mathrm{Globule}} + \int d\mathbf{r}\, f(y(\mathbf{r}))$, where $F_{\mathrm{Globule}} = (b_0/2)N\rho\nu + (c/6)N(\rho\nu)^2$ is the constant free energy for the globule and

$$f(y(\mathbf{r})) = \frac{m-1}{m}\frac{3}{2}\rho k_B T \ln\left[\left(\frac{2}{A\sigma^2}\right)y+1\right] - (m-1)\frac{\beta b^2}{4}2^{-3/2}\nu\rho^2 \times\left[\left(\frac{y}{y+1}\right)^{3/2} - \frac{45}{128}\sigma^2\frac{(\nabla y)^2}{(y+1)^{7/2}}\right] \tag{40}$$

is the inhomogeneous free energy density. The surface tension is proportional to b^2 and originates from the randomness of the interactions. Since the monomer density does not change significantly in a collapsed phase of a model with excluded volume, we ignore the derivative of the density. The complex effect of these two order parameters can be taken into account in a more elaborate theory describing a more complex instanton with two field variables. This may be important for natural proteins. In the functional, m, y, and ρ are functions of $\mathbf{r}$. The former two play the main roles in glassy behavior.

Inhomogeneous saddle point solutions of the free energy functional in the replica formulation give a microscopic theory of the barrier analogous to the KW result for $T_A > T > T_K$. We can utilize the same droplet method as in the previous section. The random interactions are integrated out and so the interface of the replicated droplet will be spherical, minimizing the surface energy. In spherical coordinates, the stationary phase condition for $y(r)$ leads to an Euler–Lagrange equation,[17] which corresponds to the Newton equation of a dissipative system, where *time* is r and a *coordinate* is y. (This is a little more complicated than before because the *mass* here depends on y.) For an infinite polymer, the appropriate solution has the boundary conditions $dy/dr|_{r=0} = 0$ and $y(\infty) = y_G$. Since the dissipation diverges at $r=0$, the solution stays at $y=0$ at the beginning of trajectory ($r \sim 0$), falls after a while with an infinitesimal initial velocity, and stops at $y=y_G$. Since the dissipation monotonically decreases with r, there is one such trajectory for each temperature. The critical radius r_c defined by the value of r, where $y(r_c) = y^{\ddagger}$, is shown as a function of temperature in Fig. 7. Figure 8 shows the critical free energy of the droplet in an infinite system as well as that for a uniform transition for a finite but large N. In these figures, we depict the results obtained by the so-called *thin wall approximation*,[17] which assumes a plane domain wall giving a free energy of the KW form. The shape of the domain wall is depicted in Fig. 9. The width of the wall is about 3σ and slightly increases as temperature increases.

For proteinlike parameters, just below T_A, the free energy barrier for reconfiguration due to a droplet in an infinite

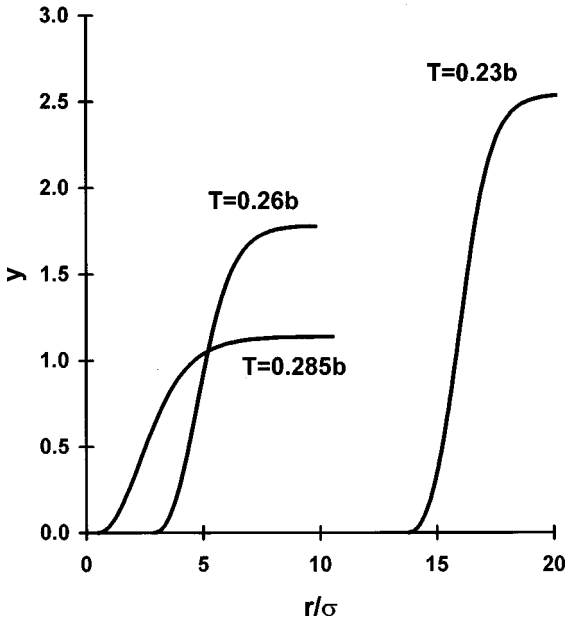

FIG. 9. The shape of the domain wall of entropic droplets at temperature $T/b=0.23$, 0.26, and 0.285. Parameters used are the same as Fig. 6.

system is higher than the barrier for a uniform transition of a polymer with a moderate size (e.g., 1000 mer). The interface for the droplet of small radius costs a considerable surface energy, reflecting the difficulty of healing the interface. Near T_A, a polymer of this size escapes from traps through a nearly uniform reconfiguration. Decreasing temperature, a localized escape mechanism begins to dominate (Fig. 8) for sufficiently large proteins, but the critical radius then increases upon further cooling until it reaches the whole size of the polymer, because the entropic driving force for transition finally disappears at T_K. Near T_K, if we take into account finite size effects in a similar way as was done for thermodynamic folding nucleus, either an exposed or embedded droplet of a size similar to the protein itself will give a critical free energy barrier. The finite size effect will modify T_K to some extent, since the saturation due to obligate freezing will occur at a different temperature for the finite protein. Our calculation yields the result that exposed or embedded droplets reduce the reconfiguration barrier at T_K for a finite system. We point out, however, finite size effects in the replica formalism are not at all straightforward to interpret, and so the calculation is still somewhat speculative near T_K.

The width of the spherical domain wall is $\sim 3\sigma$. This is not much smaller than the radius of the smaller lattice models for proteins. The thin wall approximation is accurate for larger droplets (lower temperature), but it underestimates the free energy for small droplets. The numerical accuracy of these results, of course, depends on how well the real system is approximated by the contact model, but the trends should be robust.

IV. DISCUSSION

A simple estimate of folding times can be obtained by combining the results of the last two sections using $\tau_F = \tau \exp \beta F^{\ddagger}$, Eq. (1).[35] This simple estimate ignores the effects of temperature on collapse and the role of ruggedness in changing the thermodynamic stability of the molten globule, so it should be considered largely illustrative. Remember there are three parameters which have the dimension of energy, T, $|\epsilon_{\mathrm{Nat}}|$, and b. We choose $|\epsilon_{\mathrm{Nat}}|$ as the unit of energy and plot τ_F for a 100-mer protein as a function of T in Figs. 10 for three different choices of the parameter b. As mentioned above, τ is the reconfiguration time which is approximated as $\tau=\tau_0$ at $T>T_A$, i.e., mode coupling effects are neglected, and by $\tau=\tau_0 \exp \beta V_b$ for $T_K<T<T_A$, where τ_0 is the microscopic time scale and takes of order 10 ns and V_b is the smaller of the barriers computed using the entropic droplet or the uniform transition routes. For the temperature below T_K, we use the constant barrier obtained from uniform transition at T_K since the barrier height is already saturated below T_K. $F^{\ddagger}$ is also taken as the smaller of the barrier computed assuming a localized folding nucleus and the uniform transition. The former is always smaller in the temperature range shown here for the 100 mer Figure 10(a) clearly exhibits a minimum folding time between the glass transition temperature $T_K=0.612$ and the folding temperature $T_F(100)=1.06$. This shape is similar to the folding times obtained computationally for the lattice model. With this choice of b, i.e., $b=3|\epsilon_{\mathrm{Nat}}|$, the temperature at which the folding time is minimal, $T_{\mathrm{min}}=0.81$ is about 76% of $T_F(100)$. For a typical protein (CI2, for example), T_F is about 350 K experimentally. An estimated T_{min} is 270 K, which differs somewhat from experiment. The minimal folding time is of order 1 μs, which is a bit too fast. The frustration for these parameters is probably too weak. For a more rugged landscape with $b=3.5|\epsilon_{\mathrm{Nat}}|$, the folding time is plotted in Fig. 10(b). Again with $T_F=350$ K, we obtain T_{min}, here corresponding to 307 K, a physiological temperature. With this parameter, the minimal folding time is of order 10 μs and the folding time at T_F is about 50 ms, which seem to be reasonable. The resulting estimate for T_F/T_K is 1.48. This is close to the value 1.6 deduced by mapping to the 27-mer simulation.[36] It is interesting to note that while for a well designed 27-mer lattice model, the protein folds fastest around T_F,[2] for larger proteins, $T_F(N)$ is not the fastest folding temperature because the folding barrier grows with $N^{2/3}$ at $T_F(N)$.[20] We also calculated the folding time using the choice $b=4|\epsilon_{\mathrm{Nat}}|$, which is plotted in Fig. 10(c). Here, we do not see significant minimum in folding time and the frustration seems to be apparently too strong. Of course, the comparison of absolute temperatures in real proteins must take into account the fact that the dominant force for folding and trapping is hydrophobicity. Hydrophobic forces have a large but not purely entropic component. We plan to return to this issue in later work.

In Sec. II, we only described a nonspecific folding nucleus with the variational formalism. Here, we touch upon the specific folding nucleus route. As mentioned above, the latter is expected to be more advantageous when only a very small nucleus is necessary to overcome the thermodynamic barrier. One way of realizing the specificity of the native interactions is to use the H_{Go} term in the Hamiltonian Eq.

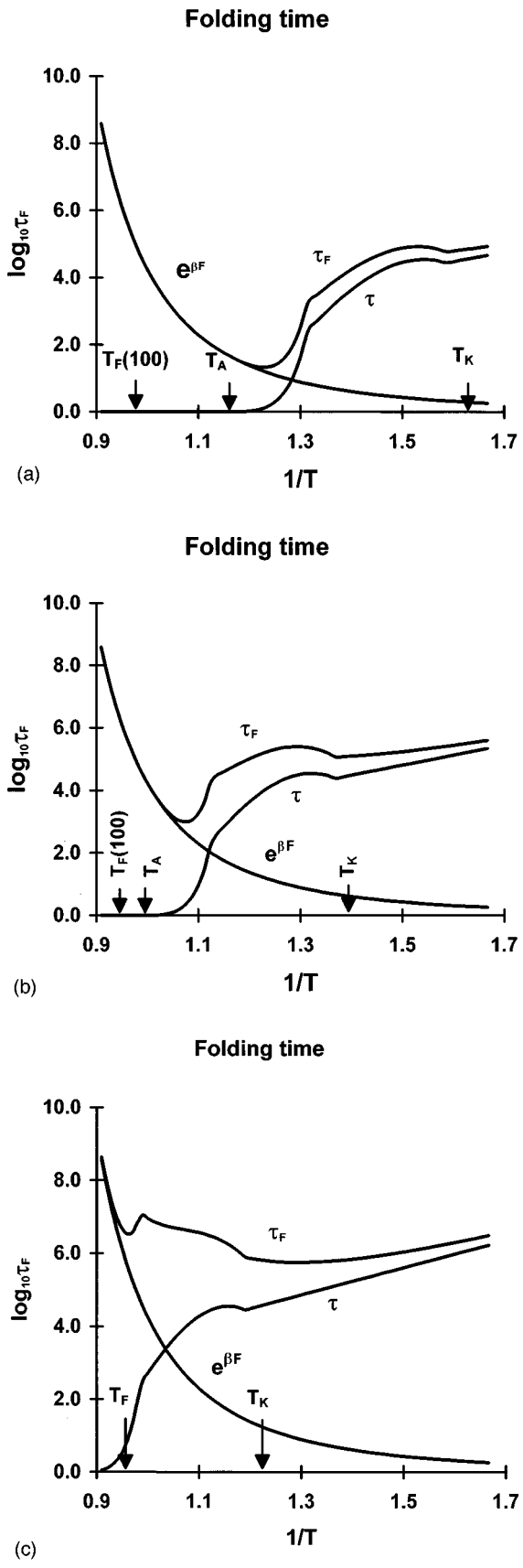

FIG. 10. Folding time of a 100-mer protein as a function of temperature. Parameters are taken from those of Figs. 1 and 6 with (a) $b=3|\epsilon_{\mathrm{Nat}}|$ (too weak frustration), (b) $b=3.5|\epsilon_{\mathrm{Nat}}|$ (a reasonable ratio), and (c) $b=4|\epsilon_{\mathrm{Nat}}|$ (too strong frustration). Energies are measured in the unit of $|\epsilon_{\mathrm{Nat}}|$.

(2), but with varying contact strength $H_{\mathrm{Go}}=\Sigma_{(\mu\nu)}^{(\mathrm{N})}b_{\mu\nu}u(\mathbf{r}_\mu-\mathbf{r}_\nu)$. $b_{\mu\nu}$ may be chosen, for example, from Miyazawa–Jernigan[37] contact energies with an amino acid sequence of a real protein. Within our variational approach, we may formulate a reference Hamiltonian for the inhomogeneous nucleus route as

$$\beta H_{\mathrm{ref}}(C_{\mathrm{Nuc}},C_{\mathrm{Rest}})=A\sum(\mathbf{r}_{i+1}-\mathbf{r}_i)^2+B\sum\mathbf{r}_i^2 \tag{41}$$

$$+C_{\mathrm{Nu}}\sum_{\mu\nu\in\mathrm{NucPairs}}(\mathbf{r}_\mu-\mathbf{r}_\nu)^2$$

$$+C_{\mathrm{Rest}}\sum_{\mu\nu\in\mathrm{RestPairs}}(\mathbf{r}_\mu-\mathbf{r}_\nu)^2, \tag{42}$$

where ''Nuc Pairs'' and ''Rest Pairs'' mean a set of contact pairs included in the nucleus and the set of the other native pairs. In the $(C_{\mathrm{Nuc}},C_{\mathrm{Rest}})$ plane, we can compute the free energy surface giving a barrier height. If the native contacts vary sufficiently in energy, a particular set of nucleus contact pairs gives significantly lower barrier than other choices. This will be a good candidate for a ''specific'' folding nucleus. We note that this estimate takes into account the entropy loss due to the formation of contacts. Detailed investigation of this approach will be presented elsewhere.

In Sec. III, we have described droplets that are local in space. There is an alternative escape route: an entropic droplet local in sequence. This can be treated using a similar reference Hamiltonian to Eq. (34), but with D_i depending on sequence number i. Straightforward calculation shows that the activation barrier for the sequentially localized droplet is proportional to the size of system N between T_A and T_K, while for droplets local in space the activation energy is independent of N except very close to T_K. Entropic droplets local in sequence, therefore, do not change the story much. Droplets local both in sequence and space correspond for glassy traps with the *foldons* of a minimally frustrated system and may be relevant when topological constraints are considered.[38]

Entropic droplets are important in the study of structural glasses, too. In the latter, many studies have been dedicated to extending the mode coupling theory (MCT). The key problem is how to quantify the thermal activation events on the rugged part of the free energy landscape. Since the MCT of structural glass in its original form does not take into account this activation at all, it applies only for temperatures above a critical value often denoted as T_c, which corresponds to T_A in our formulation. Bouchaud *et al.*[39] recently extended the MCT into the temperature range below the calorimetric glass transition temperature T_g, which corresponds to T_K in the present work. In this temperature range, thermal hopping is already frozen so that activated events need not be taken into account. As described above, thermal activation governs the equilibrium dynamics in the range $T_A>T>T_K$, which is indeed experimentally the most relevant range for clarifying the ideal glass transition. Extended MCTs put rates of hopping phenomenologically into the theory and fit them with experiments. While the results are

modestly successful, they do not represent a complete microscopic theory until the hopping rates are calculated in the theory. The entropic droplets presented here give the barrier for the hopping. Examining our analysis reveals that nearly the same formalism may be applied to the structural glass problem, too. A technical problem is that the replica formalism can only be applied for the system with the quenched randomness, which is not *a priori* present in the structural glasses. There is already much evidence, however, that quenched randomness is not necessary for most of the phenomena found in the spin glass models to be relevant.

The explicit droplet solutions discussed here are oversimplified. For structural glass and Potts glasses, scaling arguments suggest that the interface has a more complex structure.[30] Wetting due to multiple states in the interface reduces the effective surface tension significantly. This leads to the Vogel–Fulcher dependence of the barrier height $\Delta F \sim (T-T_K)^{-1}$. We have not yet succeeded in quantifying this wetting phenomenon in the replica instanton formalism. Inhomogeneous states of a polymer (and short range Potts-type models, in general) may not, rigorously speaking, be described by the simple one level replica symmetry breaking scheme but require a $P(q)$ with finite width peaks. A treatment of the interface like that used for the short range Sherrington–Kirkpatrick model[31] may incorporate the wetting effect.

V. CONCLUSION

We have studied two kinds of localized excitations which are especially relevant to folding of larger proteins: A nonspecific homogeneous folding nucleus and entropic droplets which give a route to the reconfiguration at temperature range between T_A and T_K. At T_F, the size of folding nucleus is of the order of a protein itself, but gets smaller in decreasing temperature. When a large nucleus is necessary for the folding, the nonspecific nucleus route is advantageous, but very small nuclei may be more specific. Near T_A, entropic droplets have broad interface, so modest size proteins escape from traps via nearly uniform reconfigurations. Relatively larger proteins, on the other hand, should reconfigure via the entropic droplet mechanism.

ACKNOWLEDGMENTS

We are grateful to Jin Wang and John Portman for useful discussions. S.T. has been supported by the JSPS both through Fellowships for Research Abroad and through Research Fellowships for Young Scientists. P.G.W. is supported by NIH Grant No. PHS 1 R01 GM44557.

APPENDIX: SIMPLE ALGEBRA FOR A FINITE SIZE EDGE NUCLEUS

Here, we just list the formula used to estimate the surface area and the volume of the folding nucleus which is either embedded in or exposed to a protein. Refer to Fig. 5 for the notation used. The surface area S_1 of type S_1,S_2 at surface S_2, and the volume V of the folding nucleus are computed as

$$S_1=4\pi R_N^2 \quad S_2=0,$$

and

$$V=4\pi R_N^3/3,$$

when $R_N<R_{\rm tot}-x$,

$$S_1=4\pi R_N^2\,\frac{R_{\rm tot}^2-(x-R_N)^2}{4xR_N},$$

$$S_2=4\pi R_{\rm tot}^2\,\frac{R_N^2-(x-R_{\rm tot})^2}{4xR_{\rm tot}},$$

and

$$V=4\pi R_N^3/3\,\frac{2-3\cos\,\theta_0+\cos^3\,\theta_0}{4}+4\pi R_{\rm tot}^3/3\,\frac{2-3\cos\,\theta_1+\cos^3\,\theta_1}{4}$$

when $R_{\rm tot}+x>R_N>|R_{\rm tot}-x|$, and

$$S_1=0, \quad S_2=4\pi R_{\rm tot}^2 \quad V4\pi R_{\rm tot}^3/3,$$

when $R_N>R_{\rm tot}+x$. Here $\cos\,\theta_0$ and $\cos\,\theta_1$ are defined in the figure.

[1] J. D. Bryngelson, J. N. Onuchic, N. D. Socci, and P. G. Wolynes, PROTEINS: Struct, Funct, Genetics. **21**, 167 (1995).
[2] N. D. Socci, J. N. Onuchic, and P. G. Wolynes, J. Chem. Phys. **104**, 5860 (1996).
[3] J. D. Bryngelson and P. G. Wolynes, Biopolymers **30** 177 (1990).
[4] L. S. Itzhaki, D. E. Otzen, and A. Fersht,J. Mol. Biol. **254**, 260 (1995).
[5] B. A. Shoemaker, J. Wang, and P. G. Wolynes, Proc. Natl. Acad. Sci. USA **94**, 777 (1997).
[6] J. N. Onuchic, N. D. Socci, Z. A. Luthey-Schulten, and P. G. Wolynes, Folding Design **1**, 441 (1996).
[7] E. I. Shakhnovich, A. Abkevich, and O. Ptitsyn, Nature (London) **379**, 96 (1996).
[8] D. Thirumalai and Z. Guo, Biopolymers **35** 137 (1995); Z. Guo and D. Thirumalai, Biopolymers **36**, 83 (1995).
[9] A. M. Gutin, V. I. Abkevich, and E. I. Shakhnovich, Phys. Rev. Lett. **77**, 5433 (1996).
[10] J. D. Bryngelson and P. G. Wolynes, Biopolymers **30**, 177 (1990); D. Thirumalai, J. Phys. I (France) **5**, 1457 (1995); P. G. Wolynes, *Proc. NATO ASI*, edited by T. Riste (Kluwer Academic, The Netherlands), in press.
[11] ''K'' stands for Kauzmann, since he suggested the relevance of the temperature where configuration entropy disappears to the static glass transition.
[12] S. Takada and P. G. Wolynes, Phys. Rev. E **55**, 4562 (1997).
[13] N. Gō, Annu. Rev. Biophys. Bioeng. **12**, 183 (1983), and references therein.
[14] A. Y. Grosberg and A. R. Khokhlov, *Statistical Physics of Macromolecules*, translated by Y. A. Atanov, (AIP, New York, 1994).
[15] M. Sasai and P. G. Wolynes, Phys. Rev. Lett. **65**, 2740 (1990); Phys. Rev. A **46**, 7979 (1992).
[16] For example, J. S. Rowlinson and B. Widom, *Molecular Theory of Capillarity* (Clarendon, Oxford, 1982).
[17] For example, S. Coleman, *Aspects of Symmetry* (Cambridge University Press, Cambridge, 1985).
[18] D. Oxtoby, in *Liquids, Freezing and the Glass Transition*, edited by D. Levesque, J. P. Hansen, and J. Zinn-Justin (Elsevier, New York, 1991), pp. 145.
[19] A. V. Finkelstein and A. Y. Badretdinov, Folding Design **2**, 115 (1997).
[20] P. G. Wolynes, Proc. Natl. Acad. Sci. USA **94**, 6170 (1997).
[21] R. R. Matheson, Jr. and H. A. Scheraga, Macromolecules **11**, 819 (1978).
[22] S. Takada and P. G. Wolynes, Prog. Theor. Phys. Suppl. **126**, 49 (1997).

[23] J.-P. Bouchaud and D. S. Dean, J. Phys. I (France) **5**, 265 (1995), and references therein.
[24] C. A. Angell, Science **267**, 1924 (1995), and other articles in the same volume.
[25] H. Frauenfelder, S. G. Sligar, and P. G. Wolynes, Science **254**, 1598 (1991).
[26] M. Mezard, G. Parisi, and M. A. Virasoro, *Spin Glass Theory and Beyond*, (World Scientific, Singapore, 1987).
[27] T. Garel and H. Orland, Europhys. Lett. **6**, 307 (1988).
[28] E. I. Shakhnovich and A. M. Gutin, J. Phys. A **22**, 1647 (1989); Biophys. Chem. **34**, 187 (1989).
[29] T. R. Kirkpatrick and P. G. Wolynes, Phys. Rev. B **36**, 8552 (1987).
[30] T. R. Kirkpatrick, D. Thirumalai, and P. G. Wolynes, Phys. Rev. A **40**, 1045 (1989); P. G. Wolynes, *Proceedings International of the Symposium on Frontiers in Science*, edited by S. S. Chan and P. G. Debrunner (AIP, New York, 1988).
[31] G. Parisi, preprint cond-mat/9411115; S. Franz, G. Parisi, and M. A. Virasoro, J. Phys. I (France) **4**, 1657 (1994).
[32] S. F. Edwards and M. Muthukumar, J. Chem. Phys. **89**, 2435 (1988).
[33] J. Kurchan, G. Parisi, and M. A. Virasoro, J. Phys. I **3**, 1819 (1993).
[34] S. Takada, J. J. Portman, and P. G. Wolynes, Proc. Natl. Acad. Sci. USA **94**, 2318 (1997).
[35] Notice in doing this we have neglected prefactors in the rate that depend on details of chain motion. They require evaluating functional determinants as in other field theories.
[36] J. N. Onuchic, P. G. Wolynes, Z. Luthey-Schulten, and N. Socci, Proc. Natl. Acad. Sci. USA **92**, 3626 (1995).
[37] S. Miyazawa and R. L. Jernigan, Macromolecules **18**, 534 (1985).
[38] A. Panchenko, Z. A. Luthey-Schulten, and P. G. Wolynes, Proc. Natl. Acad. Sci. USA **93**, 2008 (1996).
[39] J. P. Bouchaud, L. F. Cugliandolo, J. Kurchan, and M. Mezard, Physica A **226**, 243 (1996).